The mechanical basis of *Drosophila* audition

Martin C. Göpfert*,[1] and Daniel Robert[1]

Institute of Zoology, University of Zurich, Winterthurerstraße 190, CH-8057 Zurich, Switzerland

[1]Present address: School of Biological Sciences, University of Bristol, Woodland Road, Bristol BS8 1UG, UK

*e-mail: m.gopfert@bristol.ac.uk

Summary

In *Drosophila melanogaster*, antennal hearing organs mediate the detection of conspecific songs. Combining laser Doppler vibrometry, acoustic near-field measurements and anatomical analysis, we have investigated the first steps in *Drosophila* audition, i.e. the conversion of acoustic energy into mechanical vibrations and the subsequent transmission of vibrations to the auditory receptors in the base of the antenna. Examination of the mechanical responses of the antennal structures established that the distal antennal parts (the funiculus and the arista) together constitute a mechanical entity, the sound receiver. Unconventionally, this receiver is asymmetric, resulting in an unusual, rotary pattern of vibration; in the presence of sound, the arista and the funiculus together rotate about the longitudinal axis of the latter. According to the mechanical response characteristics, the antennal receiver represents a moderately damped simple harmonic oscillator. The receiver's resonance frequency increases continuously with the stimulus intensity, demonstrating the presence of a non-linear stiffness that may be introduced by the auditory sense organ. This surprising, non-linear effect is relevant for close-range acoustic communication in *Drosophila*; by improving antennal sensitivity at low song intensities and reducing sensitivity when intensity is high, it brings about dynamic range compression in the fly's auditory system.

Key words: acoustic communication, auditory tuning, biomechanics, bioacoustics, chordotonal organ, courtship, dynamic range compression, ear, insect, antenna, hearing, song, Johnston's organ, mechanosensation, non-linearity, *Drosophila melanogaster*.

Introduction

The antennae of *Drosophila melanogaster* are known to serve at least two functions. Apart from forming olfactory organs (for a review, see Carlson, 1996), they also constitute hearing organs sensitive to the particle velocity component of airborne sound (for a review, see Eberl, 1999). Indeed, in addition to olfactory and visual cues, the emission and perception of acoustic signals play prominent roles in the mating behaviour of these fruit flies (for a review, see Greenspan and Ferveur, 2000). The signals, colloquially known as 'love songs', are generated by wing vibration. As soon as a male fly has approached and oriented towards a female, it extends and vibrates one of its wings, thereby emitting a species-specific song. This sound enhances the female's receptivity to copulation and, thus, facilitates mating (for reviews, see Bennet-Clark, 1971; Ewing, 1983; Hall, 1994; Greenspan and Ferveur, 2000).

Since the discovery of acoustic signalling in fruit flies (Shorey, 1962), the generation of these signals has been extensively studied at the behavioural, physiological, genetic and molecular levels (for reviews, see Bennet-Clark, 1971; Ewing, 1983; Greenspan, 1997; Greenspan and Ferveur, 2000; Hall, 1994, 1998; Yamamoto et al., 1997). Surprisingly little, however, is known about the sensory aspects of this acoustic communication system. A series of early studies, mostly dating from the 1960s and 1970s, established that the antennae of *Drosophila* to serve as 'love song' detectors (Ewing, 1983); as in most flies, the antennae of *Drosophila* are characteristically composed of three segments including (from proximal to distal) the scape, the pedicel and the funiculus. The latter carries an elongated and branched lateral process, the antennal arista (Fig. 1). Ablation of either the funiculus or only the arista results in a severely reduced receptivity, indicating that the antennal arista and possibly the funiculus are involved in sound perception, presumably by constituting the sound receiver proper (Manning, 1967; von Schilcher, 1976). This idea was supported by the reduced sexual receptivity of antennal mutants (e.g. *aristaless*) (Burnet et al., 1971) and by the stroboscopic observation of antennal vibrations induced by intense sound (Manning, 1967; Bennet-Clark, 1971). Electrophysiological recordings, in turn, finally demonstrated that Johnston's organ, a mechanosensory chordotonal organ in the pedicel of the antenna, serves as the auditory sensory organ (Ewing, 1978). Taken together, these early studies documented the auditory function of *Drosophila* antennae. More detailed information about the underlying anatomical, biomechanical and neurophysiological mechanisms, however, remained
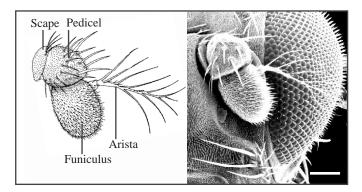
Fig. 1. The *Drosophila melanogaster* antenna. Schematic drawing (left) and scanning electronmicrograph (right). Each antenna is composed of three segments, the scape, the pedicel and the funiculus, the latter carrying the feather-like arista. The drawing by P. Bryant was reproduced with permission from FlyBase (1999). Scale bar (right panel), 0.1 mm.

elusive, presumably reflecting the technical limitations arising from the small size of the flies' antennal hearing organs.

Recently, audition in *Drosophila melanogaster* has attracted renewed interest. Because of its amenability to genetic and molecular research, the species is currently used as a model organism to examine the fundamental processes underlying mechano- and auditory transduction (Kernan et al., 1994; Kernan and Zuker, 1995; Eberl et al., 1997, 2000). Research in this context has made considerable progress and led to the identification of several auditory-relevant genes (Kernan et al., 1994; Eberl et al., 1997, 2000; Eddison et al., 2000; Walker et al., 2000; Chung et al., 2001). Now, complementary information about the biomechanical events underlying *Drosophila* audition is needed to evaluate comprehensively the consequences of mutant defects on the auditory performance of the fly (Eberl et al., 2000; Göpfert and Robert, 2001a).

The present account focuses on the first steps in audition in *Drosophila melanogaster*, i.e. on the conversion of acoustic energy to mechanical vibrations and on the transmission of vibration to the sensory organ. Using computer-controlled laser Doppler vibrometry in conjunction with anatomical investigations and acoustic near-field measurement techniques, the structural and mechanical bases of *Drosophila* audition are examined. The main aim of this study is to establish the fundamental mechanical characteristics of the antennal hearing organs of wild-type flies and, thus, to provide a framework for comparative analyses in auditory mutants. To investigate the antenna's suitability as a detector of courtship song, the mechanical measurements are supplemented by acoustic analysis of these songs.

Materials and methods

Animals

Wild-type *Drosophila melanogaster*, Oregon R strain, were reared on standard medium at 22–25 °C. For mechanical examination, the flies were briefly anaesthetized with CO_2, and the wings and legs were removed. Subsequently, the animals were waxed dorsum-down on the end of a wooden rod 5 mm in diameter and 10 cm in height. The compound eyes were waxed to the thorax to stabilize the head. Only one antenna was examined per animal. The arista of this antenna was oriented perpendicular to both the axis of measurement and the direction of sound propagation, an arrangement that provided the highest vibration amplitudes and reproducible positioning (Fig. 2A). The corresponding angle between the animal's longitudinal axis and the axis of measurement (typically 20–25 °; Fig. 2B) was adjusted by turning the holder with the animal. All experiments were carried out on a vibration isolation table (TMC 78-443-12) at room temperature (24–26 °C).
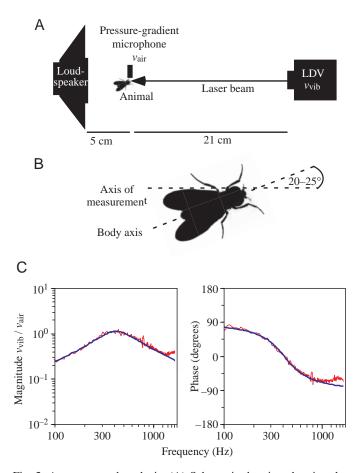

Fig. 2. Apparatus and analysis. (A) Schematic drawing showing the arrangement of the loudspeaker, the animal, the pressure-gradient microphone and the laser Doppler vibrometer (LDV). The vibration velocity v_{vib} was assessed *via* the LDV, the particle velocity v_{air} *via* the microphone. (B) Detail from A depicting the animal's orientation during the measurements (in contrast to the picture shown, the animal's wings and legs were removed for experiments). (C) Comparison between the measured velocity response of an arista (red trace) and the fitted function of a simple harmonic oscillator (blue trace). Magnitude (left panel) and phase (right panel) responses are shown. The fitted function is described by f_0=394 Hz, Q=1.24 and v_{vib}/v_{air} at f_0=1.13, where f_0 is the resonance frequency and Q is the quality factor.

Mechanical measurements

Antennal vibrations were analyzed in response to acoustic excitation with pseudo-random noise signals (frequency range 100–1500 Hz). The acoustic signals were generated by a Stanford Research System Network analyzer (Stanford Research Systems, model SR 780), passed through a step attenuator (custom-built), amplified (dB-Technologies, model PL 500) and fed to a loudspeaker (Uher, model UL-1302, 13 cm in diameter, fitted with a baffle 25 cm in diameter).

Sound-induced mechanical vibrations were examined by means of input/output analyses based on simultaneous measurements of the vibration velocity v_{vib} of the antennal structures and the particle velocity v_{air} in the surrounding air (Fig. 2A). v_{vib} was assessed using a microscanning laser Doppler vibrometer (Polytec, model PSV 200) with an OFV-055 scanning head. To facilitate vibration measurements coaxial to the direction of sound propagation, a linear arrangement of the laser, the animal and the loudspeaker was chosen, with the laser pointing to the centre of the loudspeaker and the experimental animal being positioned between the loudspeaker and the laser vibrometer (Fig. 2A). The distances between the loudspeaker and the animal and between the animal and the laser vibrometer were 5 and 21 cm, respectively, the latter corresponding to the focal length of the laser optics. The laser beam (approximately 5 μm spot diameter) was positioned with a spatial accuracy of approximately 1 μm using an OFV-3001-S vibrometer beam controller, and the spot position was monitored online *via* the coaxial video system of the scanning head. It is noteworthy that both the sensitivity of the vibrometry apparatus and the high accuracy of beam positioning obviated the use of reflecting beads on any of the measured structures.

To monitor v_{air}, a miniature Emkay NR 3158 pressure gradient microphone (distributed by Knowles Electronics Inc., Itasca, Illinois, USA) was used in combination with an integrating amplifier (modified after Bennet-Clark, 1984). The dimensions of the NR 3158 microphone are 5.6 mm×4.0 mm×2.2 mm, the latter corresponding to the spacing between the microphone's ports. The microphone shows a symmetrical figure-of-eight pattern of directivity. Sensitivity is maximal when the microphone's diaphragm faces the incident sound and drops by 42 dB (at a frequency of 500 Hz) when turned through 90°. Turning the microphone through 180° so that its back surface faced the incident sound does not affect sensitivity (change in sensitivity less than ±0.5 dB at 500 Hz) and results in the expected 180° phase shift in the microphone's response.

The voltage output of this microphone was calibrated against the output of a precision pressure microphone (Bruel & Kjaer, type 4138) under far-field conditions and, thus, could be directly converted to the corresponding particle velocity. Far-field calibration against the pressure microphone also confirmed the output of the pressure gradient microphone to be flat within ±0.6 dB at frequencies between 100 and 1500 Hz. During the vibration measurements, the pressure gradient microphone was positioned next to the antenna (distance 0.5 cm) with its diaphragm oriented perpendicular to the direction of sound propagation (Fig. 2A) so that its response was maximal. Control measurements of sound-induced antennal vibrations in the presence and absence of the microphone confirmed that the microphone did not affect the sound field at the position of the antenna. The sound field has been described by Göpfert et al. (1999).

To analyse the data, the laser and microphone signals were digitized at 12.5 kHz using an Analogic 16 Fast A/D board. To produce frequency spectra, groups of 3–5 windows, each 120 ms in length, were collected, subjected to the Fast Fourier transform using a rectangular window, and subsequently averaged. Frequency spectra were estimated with a resolution of 6.25 Hz. To measure mechanical responses, the laser signal was normalized to the microphone signal by computing a transfer function, calculated as the cross-power spectrum between the laser and microphone signals divided by the auto-power spectrum of the latter. Magnitude information was subsequently converted to the corresponding v_{vib}/v_{air} value. Data reliability was assessed by computing coherence functions. Resonance parameters (i.e. the resonance frequency f_0, the quality factor Q and the dimensionless mechanical sensitivity v_{vib}/v_{air} at f_0) were determined by means of a least-squares fit according to a simple harmonic oscillator model using a software package in Microsoft Excel 7.0 (Frank et al., 1999). By fitting the function to the complex data, both the magnitude and the phase information were taken into account. Consistently, the model produced a near-perfect fit to the data (Fig. 2C).

Courtship song recordings

Courtship songs were recorded using conventional methods (Bennet-Clark, 1984). In brief, couples of previously isolated males and females were introduced into a small Perspex tube (10 mm diameter) containing the pressure gradient microphone at its centre. As soon as the male started to sing, its song was recorded. The signals were stored on DAT and subsequently resampled at a rate of 10 kHz for offline analysis. The frequency composition of the songs was evaluated on the basis of 40 ms time traces centred on the onset of single song pulses. Per animal, 20–30 such time-traces were averaged and subsequently converted to the frequency domain using the software Canary (rectangular time window, 0% overlap, 4.4 Hz frequency resolution).

Anatomy

The histological methods used to examine the auditory anatomy of flies have been described (Robert and Willi, 2000). The animals were cooled to 4°C prior to decapitation. The heads were subsequently fixed in 3% glutaraldehyde and embedded in Spurr's medium. Serial sections, 5 μm in thickness, were conventionally stained with Methylene Blue and examined under a light microscope (Axiophot; Zeiss). For documentation, the sections were digitized using an on-chip integration digital camera (ProgRes; Karton Electronics).

Results

Auditory anatomy

It has been proposed that the distal region of the *Drosophila* antenna (the pedicel and the funiculus bearing the arista) is relevant for audition. The pedicel comprises Johnston's organ, the auditory sensory organ, whereas the funiculus with the arista appear to be involved in sound reception (Manning, 1967; Bennet-Clark, 1971; Ewing, 1978; Eberl et al., 2000). With respect to their anatomical coupling (Fig. 3), these two antennal segments are arranged like a 'key and lock'. In longitudinal sections (Fig. 3A), the pedicel is deeply invaginated in its distal region, forming an apical pit.
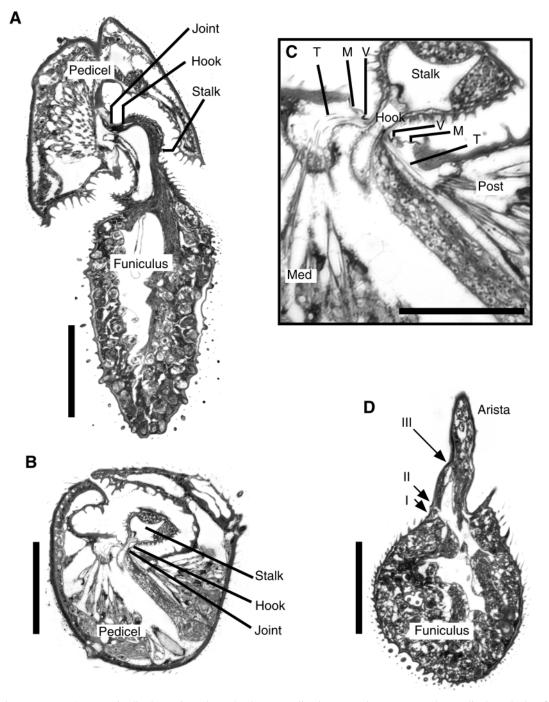

Fig. 3. Antennal anatomy. (A) Longitudinal section through the two distal antennal segments, the pedicel and the funiculus. The pedicel/funiculus joint, the funicular hook and the funicular stalk are depicted. (B) Cross section through the pedicel at the level of the pedicel/funiculus joint. (C) Detail from B showing the medial (Med) and posterior (Post) groups of receptors, their distal threads (T), the 'V'-shaped sites to which the threads attach (V) and the membrane (M) that suspends the flagellar hook in the pedicel. (D) Cross section through the funiculus at the level of the insertion of the arista. Connections between the funiculus and the arista (I) and between the three sub-elements that make up the arista (II, III) are depicted. Scale bars, 50 µm (A,B,D) and 25 µm (C).
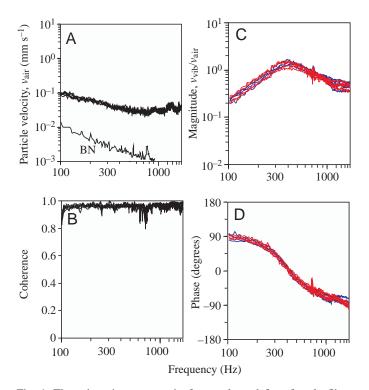
Fig. 4. The arista tip response in four male and four female flies. (A) Stimuli: superimposed frequency spectra of the acoustic random-noise stimulus at the position of the antenna during vibration measurements in eight animals and a spectrum of the background noise (BN). (B) Data reliability: frequency spectra of the coherence between the laser and the microphone signals during the same eight vibration measurements. Coherence can range between 0 and 1, with a value of 1 indicating the absence of unrelated noise. (C) Superimposed magnitude responses of the eight arista tips examined (males, blue traces; females, red traces). A response magnitude of unity ($v_{vib}/v_{air}=1$), where v_{vib} is the vibration velocity and v_{air} is the particle velocity, means that arista tip and air particles move at the same velocity. (D) Corresponding phase responses. A phase angle of $+90°$ means that v_{vib} leads v_{air} by a quarter of an oscillation cycle.

Proximally, the club-shaped antennal funiculus bears a thin stalk. This stalk fits into the apical pit of the pedicel. Close to its proximal end, the stalk bears a short process, the funicular hook. The hook is oriented perpendicular to the longitudinal axis of the funiculus and contains the funicular trachea and nerve (Fig. 3A). It projects anteriorly and joins the cuticle of the pedicel's pit. This connection constitutes the pedicel/funiculus joint and, notably, is the only anatomical connection between the pedicel and the funiculus (Fig. 3A–C) (see also Eberl et al., 2000).

The pedicel of the antenna is almost filled by scolopidia, the multi-cellular mechanoreceptor units of Johnston's organ. These scolopidia are amphinematic, comprising a distal tube that extends into a distal thread (for classification and terminology, see Moulins, 1976; McIver, 1985). As seen in cross sections (Fig. 3B,C), the funicular nerve separates Johnston's organ into two distinct groups of scolopidia, a

medial and a posterior group. Both groups project to the pedicel/funiculus joint. The tubes of the scolopidia are embedded in the hypodermis which, in the joint region, is detached from the cuticle (Fig. 3A–C). Only the distal threads pass through the hypodermis. Reflecting the different orientations of the two groups of scolopidia, the threads of the posterior series are nearly straight, whereas those of the medial series are strongly bent. As a result, all the receptors attach with their threads to the lateral sides of the joint and, hence, perpendicular to the hook (Fig. 3C). 'V'-shaped rims of specialized cuticle, identified by their strong staining with Methylene Blue, serve as attachment sites. These rims, which are part of the funiculus and are located on either side of the funicular hook, are flexibly suspended by thin membranes formed by the adjacent cuticle of the pedicel (Fig. 3C).

The arista connects to the funiculus *via* a ring of specialized cuticle that stains strongly with Methylene Blue (Fig. 3D). Two more rings occur further distally, dividing the arista in two basal parts and an elongated, distal part. All these connections lack membranous regions of cuticle as found at the pedicel/funiculus joint and, in addition, lack mechanoreceptors (see also Foelix et al., 1989).

Arista tip response

The mechanical response characteristics of the antennal structures to a quantified and reproducible pseudo-random noise stimulus were examined (Fig. 4A). The intensity characteristics of this stimulus, measured as v_{air}, were frequency-dependent. At frequencies between 100 and 1000 Hz, v_{air} decreased by approximately 3 dB octave^{-1}. In absolute terms, the amplitude of v_{air} was $±0.1$ mm s^{-1} at 100 Hz and $±0.03$ mm s^{-1} at 1000 Hz [corresponding to 63 dB and 53 dB root mean square (rms), re. $5×10^{-8}$ m s^{-1}, respectively]. These intensities were sufficient to obtain highly coherent vibration measurements (Fig. 4B).

Arista tip responses measured at the most distal part of the arista were remarkably uniform among animals. Examination of four male and four female aristae revealed a low inter-individual variability and no apparent sex differences. Consistently, a single resonance occurred in the range of frequencies examined. This resonance manifest itself as a peak in the magnitude response (Fig. 4C) accompanied by a shift in the phase response (Fig. 4D). As expected for the velocity response of a second-order system, the phase between the v_{vib} and v_{air} characteristically shifted from $+90$ to $–90°$ at a frequency around resonance. Only at f_0 were v_{vib} and v_{air} in phase. Individual values of f_0 varied between 405 and 445 Hz ($426±16$ Hz; mean $±1$ S.D.). The quality factor Q ranged between 1.1 and 1.3 ($1.2±0.1$). At f_0, mechanical sensitivity v_{vib}/v_{air} reached its maximum, ranging between 1.1 and 1.5 ($1.3±0.2$) for the eight aristae examined. According to these response characteristics, the arista tips of male and female antennae are moderately tuned to frequencies around 425 Hz, with the maximum vibration velocity slightly exceeding the particle velocity in the surrounding air.

Vibrational patterns

To be relevant for audition, sound-induced vibrations of the arista tip need to be transmitted to the funiculus and then to the receptors in the pedicel. Vibration measurements at different positions on the arista (Fig. 5A, left panel) revealed that the resonance observed at the tip extends along the entire length of the arista. Apart from a continuous approximately 10-fold drop in the response magnitude from the tip to the base, the shapes of the magnitude responses (Fig. 5B, left panel) and the phase responses (Fig. 5C, left panel) were almost identical for all measurement points. Hence, the three elements that make up the arista (Fig. 3D) do not vibrate relative to each other; they are stiffly coupled. The entire arista can be considered to move as a stiff rod when stimulated acoustically.

Comparative vibration measurements taken at the base of the arista and on the lateral edge of the funiculus demonstrate that these two antennal parts are also stiffly connected. The resonance observed on the arista could be detected at the site of the arista/funiculus connection (Fig. 5B, left panel, lowest curve) and on the lateral edge of the funiculus (Fig. 5, middle panel, red circles and curves). At both measurement sites, the responses exhibited almost identical magnitude and phase characteristics, demonstrating that the arista does not vibrate relative to its insertion on the funiculus. Consequently, the arista and the funiculus constitute a single mechanical entity.

The resonance observed on the lateral edge of the funiculus did not extend to its central region. Here, vibrations were hardly detectable and coherent measurements could not be obtained (data not shown). When the laser beam was positioned on the opposite, medial edge of the funiculus, however, the resonance built up again (Fig. 5, middle panels, blue circles and curves). Response magnitudes along opposite funicular edges were similar, with a maximum sensitivity v_{vib}/v_{air} of around 0.15 (Fig. 5B, middle panel). The response phases, however, were shifted by 180° within the entire range of frequencies examined (Fig. 5C, middle panel). This means that the two opposite edges of the funiculus move in opposite directions. The 180° phase shift, together with the equal response magnitudes obtained along the two funicular edges and the absence of vibrations in the central funicular region, is an unambiguous indication that the funiculus rotates about its longitudinal axis in the presence of sound.

The rotation of the funiculus does not extend to the pedicel. Consistently, vibration magnitudes obtained from different locations on the pedicel were much lower than those observed on the funicular edges, and these minute vibrations were not coherent with the stimulus (Fig. 5, right panels, green circles and curves). Comparably low-amplitude vibrations were also detected on the compound eyes (Fig. 5, right panels, orange circle and curves), confirming that the pedicel of the antenna does not undergo vibration relative to the head. Consequently, only the funiculus and the arista vibrate in response to sound.

Intensity characteristics

The analysis applied describes the antenna's mechanical response completely, provided that the system is linear. The responses of both funiculus and arista, however, exhibit a considerable degree of non-linearity that results in an intensity-dependent tuning. To evaluate this non-linear effect, the response of individual arista tips was measured at different stimulus intensities. The intensity of the random-noise stimulus depicted in Fig. 4A was varied in 3 dB steps over a range of 36 dB (Fig. 6A). The corresponding absolute amplitudes of v_{air}
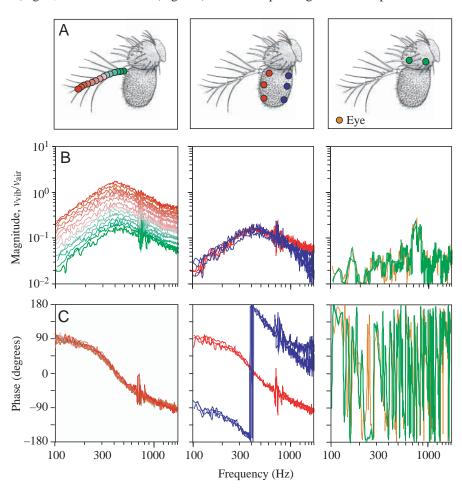

Fig. 5. Mechanical responses measured on different parts of a female arista (left panels), funiculus (middle panels) and pedicel (right panels, including one measurement from the compound eye). Measurement points (A), magnitude responses (B) and phase responses (C) are shown. For colour conventions, see A. The drawings by P. Bryant, used to depict the measurement points, were reproduced with permission from FlyBase (1999). v_{vib}/v_{air} is the response magnitude, where v_{vib} is the vibration velocity and v_{air} is the particle velocity.

ranged between ±0.03 and ±1.8 mm s⁻¹ at 100 Hz (53–88 dB re. 5×10⁻⁸ m s⁻¹) and between ±0.007 and ±0.5 mm s⁻¹ at 1000 Hz (41–77 dB re. 5×10⁻⁸ m s⁻¹).

With increasing stimulus intensity, the peak in the magnitude response and the associated zero crossing in the phase response shifted continuously towards higher frequencies (Fig. 6B,C). As shown by measurements on two male and two female aristae, this effect occurred reliably in
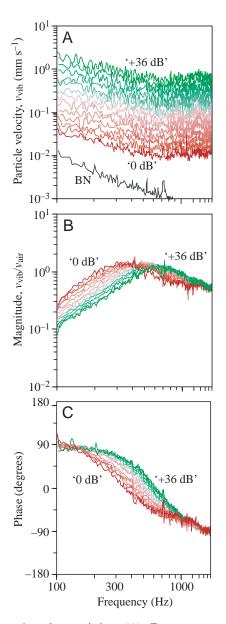

Fig. 6. Intensity characteristics. (A) Frequency spectra of the acoustic random-noise stimuli. Intensity was varied in steps of 3 dB over a total range of 36 dB. '0 dB' (red) depicts the stimulus of lowest intensity, '+36 dB' (green) the stimulus of highest intensity. (B) Superimposed magnitude responses of an individual arista tip to the stimuli depicted in A. (C) Corresponding phase responses. For colour conventions, see A. v_{vib}/v_{air} is the response magnitude, where v_{vib} is the vibration velocity and v_{air} is the particle velocity. BN, background noise.

animals of both sexes (Fig. 7A). Within the range of intensities examined, f_0 shifted from approximately 360 to 620 Hz with an average increase of 7.3 Hz dB⁻¹ (linear regressions: slopes 7.1–7.6 Hz dB⁻¹, r^2-values 0.98–1; $P<0.001$; Spearman's rank correlation, one-tailed significance) (Fig. 7A). This shift was accompanied by a slight decrease in sensitivity v_{vib}/v_{air} at f_0 (linear regressions: slopes –0.004 to –0.007 dB⁻¹, r^2-values 0.3–0.7; $P<0.01$; two-tailed significance). Tuning sharpness Q, however, remained unaffected (r^2-values <0.2, $P>0.5$) (data not shown).
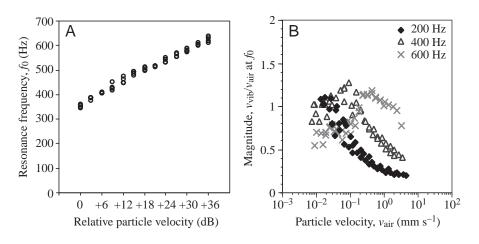
Corresponding non-linear effects were observed when the arista tip vibrations were measured in response to continuous pure tones of different intensities (Fig. 7B). Intensity/response functions obtained in this way exhibited a considerable degree of non-linearity that became apparent when v_{vib}/v_{air} at the stimulus frequency was plotted against the corresponding v_{air} (Fig. 7B). Here, the data points were not parallel to the intensity axis, as would be the case for a linear system but, instead, exhibited a sensitivity maximum at specific intensities. In accordance with the intensity-dependent resonance observed in the responses to random noise (Fig. 6), the sensitivity varied with the frequency of the pure tone. The higher the tone frequency, the higher the intensity at which the maximum occurred (Fig. 7B), reflecting the increase in f_0 (Fig. 7A).

Courtship songs

Courtship songs of *Drosophila melanogaster* consist of two components, sine songs and pulsed songs (Ewing, 1983). Pulsed songs are produced more regularly, are higher in intensity and constitute the song component that has been demonstrated to increase female receptivity (Ewing, 1983; Crossley et al., 1995). Accordingly, the analysis was focused on this song component. In the present recordings, the songs always consisted of trains of evenly spaced sound pulses (Fig. 8A), each pulse consisting of one dominant, high-amplitude oscillation cycle (Fig. 8B). The duration of this cycle, measured on the basis of at least 20 averaged pulses per individual ($N=5$), varied between 4.8 and 6 ms. In agreement, the frequency spectra of these pulses revealed maxima at the corresponding frequencies, i.e. between 160 and 210 Hz (Fig. 8C). The high-frequency roll-off in the spectra was steep, with amplitude decreasing by approximately 15 dB octave⁻¹.

Discussion

As the first step in auditory processing, the coupling between acoustic stimuli and the auditory receptors is a central issue in understanding the mechanosensory mechanisms underlying audition. This study elucidates the coupling for the minute antennal hearing organs of wild-type *Drosophila melanogaster*. In addition to documenting the antenna's response characteristics, its unusual pattern of rotation, its level-dependent tuning and its rather surprising suitability as a 'love song detector', the present experimental approach establishes a sensitive and non-invasive method that may help to evaluate mutant defects in mechanoreception.

Fig. 7. (A) The frequency f_0 of the resonance measured at the arista tips of two males and two females as a function of the relative particle velocity of the random-noise stimuli (for corresponding absolute particle velocities, see Fig. 6A). f_0 increases linearly with stimulus intensity. (B) Intensity-dependent response magnitudes of two male and two female arista tips to pure-tone stimulation at different frequencies. The responses exhibit maxima at frequency-specific intensities. v_{vib}/v_{air} is the response magnitude, where v_{vib} is the vibration velocity and v_{air} is the particle velocity.

Coupling mechanisms

Our measurements demonstrate that the distal parts of the *Drosophila* antenna serve as the sound receiver. The funiculus and the arista are stiffly coupled and constitute a single mechanical entity. Only this entity undergoes significant and coherent vibration when stimulated acoustically; it must be directly driven by sound, converting acoustic energy into mechanical vibrations.

The mechanical entity formed by the funiculus and the arista exhibits an unconventional rotatory pattern of vibration. This rotation is a consequence of the asymmetric antennal structure: because sound acts on both sides of the rotational axis, only a structural asymmetry can prevent equilibrium between clockwise and counterclockwise torque. In *Drosophila*, the arista breaks antennal symmetry. Inserted radial to the rotational axis of the funiculus, the arista constitutes a moment arm, enlarges the effective surface area and, thus, determines the torque exerted by sound. Given this vibrational pattern, it is not surprising that arista ablation reduces acoustically evoked behavioural responses by approximately the same amount as removal of the entire arista/funiculus complex (Manning, 1967).

Being surrounded by the pedicel, the proximal region of the funiculus is not accessible to direct mechanical examination. Our anatomical investigation, however, clearly illustrates that this proximal region focuses mechanical vibrations onto the auditory receptors and counterbalances the asymmetry introduced by the arista. The funicular stalk is oriented coaxial to the rotational axis. Hence, it will join the rotation of the free, distal region of the funiculus, thereby mediating the downstream transmission of rotation. The funicular hook, however, is oriented radial to the rotational axis; it thus balances the asymmetry introduced by the arista. Like the arista, the hook will undergo predominantly translatory movements during funicular rotation. The direction of these movements will be tangential to the rotational axis of the funiculus – a pattern of movement that is facilitated by articulating membranes at the pedicel/funiculus joint. The hook's vibration will then maximally stretch and compress the auditory receptors, which all attach perpendicular to the sides of the hook. Finally, the two groups of receptors attaching to
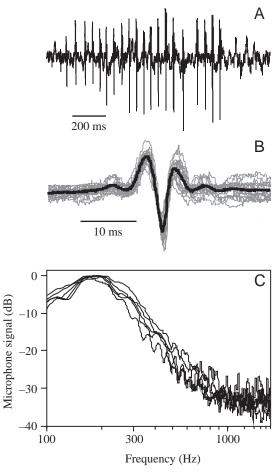

Fig. 8. Courtship songs. (A) Time trace of a song consisting of a series of 20 sound pulses. (B) Superimposed (grey traces) and averaged (black trace) time traces of the pulses shown in A. (C) Frequency spectra calculated on the basis of 20–30 averaged pulses (as shown in B) recorded from five male *Drosophila melanogaster*.

opposite sides of the hook will be stimulated in an alternate manner, a scenario that is supported by the harmonic structure of the compound electrical response of Johnston's organ (Eberl et al., 2000). Taken together, the anatomy of the funiculus and the pedicel/funiculus joint guarantees receptor activation that

compares with that of other insect chordotonal organs (Keil, 1997), despite the unusual rotational pattern of funicular vibration.

Response characteristics

According to its mechanical response characteristics, the arista/funiculus complex can be described as a moderately damped simple harmonic oscillator. Remarkably, this oscillator exhibits a considerable degree of non-linearity that does not simply reflect overloading during intense stimulation, but occurs within a wide range of intensities. As shown here, f_0 increases continuously with intensity, whereas tuning sharpness and sensitivity at f_0 are not affected or only weakly affected. Taken together, such intensity characteristics demonstrate the presence of a non-linear stiffness, a type of non-linearity that differs from the non-linear damping known from the response of vertebrate auditory systems (Dallos, 1996) and mosquito antennal hearing organs (Göpfert and Robert, 2001b). The non-linear damping observed in vertebrates and mosquitoes involves negative damping introduced by an additional power source, i.e. the active motility of the auditory receptors (Dallos, 1996). This negative damping opposes the ear's passive damping in an intensity-dependent way. Non-linear stiffness as observed in *Drosophila* may also be introduced actively. Alternatively, it may result from a passive stiffening of the auditory receptors or the cuticular components that make up the pedicel/funiculus joint. Further investigations, especially in auditory mutants (Eberl et al., 2000), promise to trace the elements in the chain of hearing, from biomechanical substrates to cellular components, that bring about auditory non-linearity in the fly and possibly active auditory mechanics.

Antennal mechanics and courtship song detection

The intensity-dependent change in f_0 is a rather surprising characteristic for an auditory filter. It results in an intensity-dependent mismatch between antennal tuning and songs. The acoustic analysis of male 'love songs' revealed a dominant frequency at approximately 200 Hz. The antenna will be tuned to this frequency only as long as intensity is low [v_{air}=17–29 dB (re. 5×10^{-8} m s^{-1}) according to a linear extrapolation, Fig. 7A]. During courtship, however, the female's antennae and the male's vibrating wing are usually only 5–2.5 mm apart, resulting in a particle velocity of around 80–95 dB (Bennet-Clark, 1971) and, according to the data presented here, in antennal resonance between 550 and 800 Hz. Acoustic communication in *Drosophila* thus operates with a frequency mismatch of up to two octaves. Several mechanisms, however, ensure signal detectability. First, acoustic communication in the fly relies on the temporal pattern of the song rather than on frequency cues (Ewing, 1983). Hence, there is no *a priori* requirement for frequency-selective hearing. Instead, the rather broad antennal tuning comes with the benefit of high temporal resolution. Second, the broad tuning, together with the short communication distance, apparently ensures that the songs induce antennal vibrations that are sufficiently large to be detected even at frequencies below antennal resonance. Third, intensity-dependent tuning may well be useful, especially in the context of close-range acoustic communication. In effect, in the acoustic near-field, the particle velocity of the sound radiated by the *Drosophila* wing drops steeply by 18 dB per doubling distance (Bennet-Clark, 1971). Hence, the flies have to cope not only with considerable sound intensities but also with considerable distance-dependent intensity fluctuations. By improving the antenna's sensitivity at low song intensities and reducing it at high intensities, the non-linear stiffness provides dynamic range compression. This mechanical compression may account for the saturation of and the decline in the neural and behavioural responses at high stimulus intensities (von Schilcher, 1976; Crossley et al., 1995; Kernan et al., 1994; Eberl et al., 2000).

References

Bennet-Clark, H. C. (1971). Acoustics of insect song. *Nature* **234**, 255–259.

Bennet-Clark, H. C. (1984). A particle velocity microphone for the song of small insects and other acoustic measurements. *J. Exp. Biol.* **108**, 459–463.

Bennet-Clark, H. C., Ewing, A. W. and Manning, A. (1973). The persistence of courtship stimulation in *Drosophila melanogaster*. *Behav. Biol.* **8**, 763–769.

Burnet, B., Connolly, K. and Dennis, L. (1971). The function and processing of auditory information in the courtship behaviour of *Drosophila melanogaster*. *Anim. Behav.* **19**, 409–415.

Carlson, J. R. (1996). Olfaction in *Drosophila*: from odor to behavior. *Trends Genet.* **12**, 175–180.

Chung, Y. D., Zhu, J., Han, Y.-G. and Kernan, M. J. (2001). *nompA* encodes a PNS-specific ZP domain protein required to connect mechanosensory dendrites to sensory structures. *Neuron* **29**, 415–428.

Crossley, S. A., Bennet-Clark, H. C. and Evert, H. T. (1995). Courtship song components affect male and female *Drosophila* differently. *Anim. Behav.* **50**, 827–839.

Dallos, P. (1996). Overview: cochlear neurobiology. In *The Cochlea* (ed. P. Dallos, A. N. Popper and R. R. Fay), pp. 1–43. New York: Springer.

Eberl, D. F. (1999). Feeling the vibes: chordotonal mechanisms in insect hearing. *Curr. Opin. Neurobiol.* **9**, 389–393.

Eberl, D. F., Duyk, G. M. and Perrimon, N. (1997). A genetic screen for mutations that disrupt an auditory response in *Drosophila melanogaster*. *Proc. Natl. Acad. Sci. USA* **94**, 14837–14842.

Eberl, D. F., Hardy, R. W. and Kernan, M. J. (2000). Genetically similar transduction mechanisms for touch and hearing in *Drosophila*. *J. Neurosci.* **20**, 5981–5988.

Eddison, M., Le Roux, I. and Lewis, J. (2000). Notch signaling in the development of the inner ear: lessons from *Drosophila*. *Proc. Natl. Acad. Sci. USA* **97**, 11692–11699.

Ewing, A. W. (1978). The antenna of *Drosophila* as a 'love song' receptor. *Physiol. Entomol.* **3**, 33–36.

Ewing, A. W. (1983). Functional aspects of *Drosophila* courtship. *Biol. Rev.* **58**, 275–292.

FlyBase (1999). The FlyBase database of the *Drosophila* genome projects and community literature. Available from http://flybase. io.indiana.edu. *Nucleic Acids Res.* **27**, 85–88.

Foelix, R. F., Stocker, R. F. and Steinbrecht, R. A. (1989). Fine-structure of a sensory organ in the arista of *Drosophila melanogaster* and some other dipterans. *Cell Tissue Res.* **258**, 277–287.

Frank, G., Hemmert, W. and Gummer, A. W. (1999). Limiting dynamics of high-frequency electromechanical transduction of outer hair cells. *Proc. Natl. Acad. Sci. USA* **96**, 4420–4425.

Göpfert, M. C., Briegel, H. and Robert, D. (1999). Mosquito hearing: sound-induced antennal vibrations in male and female *Aedes aegypti. J. Exp. Biol.* **202**, 2727–2738.

Göpfert, M. C. and Robert, D. (2001a). The key to *Drosophila* audition. *Nature* **411**, 908.

Göpfert, M. C. and Robert, D. (2001b). Active auditory mechanics in mosquitoes. *Proc. R. Soc. Lond. B* **268**, 333–339.

Greenspan, R. J. (1997). A kinder, gentler genetic analysis of behavior: dissection gives way to modulation. *Curr. Opin. Neurobiol.* **7**, 805–811.

Greenspan, R. J. and Ferveur, J. F. (2000). Courtship in *Drosophila. Annu. Rev. Genet.* **34**, 205–232.

Hall, J. C. (1994). The mating of a fly. *Science* **264**, 1702–1714.

Hall, J. C. (1998). Genetics of biological rhythms in *Drosophila. Adv. Genet.* **38**, 135–184.

Keil, T. A. (1997). Functional morphology of insect mechanoreceptors. *Microsc. Res. Tech.* **39**, 506–531.

Kernan, M., Cowan, D. and Zuker, C. (1994). Genetic dissection of mechanosensory transduction: mechanoreception-defective mutants of *Drosophila. Neuron* **12**, 1195–1206.

Kernan, M. and Zuker, C. (1995). Genetic approaches to mechanosensory transduction. *Curr. Opin. Neurobiol.* **5**, 443–448.

Manning, A. (1967). Antennae and sexual receptivity in *Drosophila melanogaster* females. *Science* **158**, 136–137.

McIver, S. B. (1976). Mechanoreception. In *Comprehensive Insect Physiology, Biochemistry and Pharmacology*, vol. 6 (ed. G. A. Kerkut and L. I. Gilbert), pp. 71–132. Oxford: Pergamon.

Moulins, M. (1976). Ultrastructure of chordotonal organs. In *Structure and Function of Proprioreceptors in Invertebrates* (ed. P. J. Mill), pp. 387–426. London: Chapman & Hall.

Robert, D. and Willi, U. (2000). The histological architecture of the auditory organs in the parasitoid fly *Ormia ochracea. Cell Tissue Res.* **301**, 447–457.

Shorey, H. H. (1962). Nature of the sound produced by *Drosophila melanogaster* during courtship. *Science* **137**, 677–678.

von Schilcher, F. (1976). The role of auditory stimuli in the courtship of *Drosophila melanogaster. Anim. Behav.* **24**, 18–26.

Walker, R., Willingham, A. and Zuker, C. (2000). A *Drosophila* mechanosensory transduction channel. *Science* **287**, 2229–2234.

Yamamoto, D., Jallon, J. M. and Komatsu, A. (1997). Genetic dissection of sexual behaviour in *Drosophila melanogaster. Annu. Rev. Entomol.* **42**, 551–585.